ORIGINAL RESEARCH

Arterial Stiffness Due to Carotid Calcification Disrupts Cerebral Blood Flow Regulation and Leads to Cognitive Deficits

Gervais Muhire, MSc;* M. Florencia Iulita, PhD;* Diane Vallerand, BSc; Jessica Youwakim, BSc; Maud Gratuze, PhD; Franck R. Petry, PhD; Emmanuel Planel, PhD; Guylaine Ferland, PhD; Hélène Girouard, PhD

***Background*—**Arterial stiffness is associated with cognitive decline and dementia; however, the precise mechanisms by which it affects the brain remain unclear.

***Methods and Results*—**Using a mouse model based on carotid calcification this study characterized mechanisms that could contribute to brain degeneration due to arterial stiffness. At 2 weeks postcalcification, carotid stiffness attenuated resting cerebral blood flow in several brain regions including the perirhinal/entorhinal cortex, hippocampus, and thalamus, determined by autoradiography ($P<0.05$). Carotid calcification impaired cerebral autoregulation and diminished cerebral blood flow responses to neuronal activity and to acetylcholine, examined by laser Doppler flowmetry ($P<0.05$, $P<0.01$). Carotid stiffness significantly affected spatial memory at 3 weeks ($P<0.05$), but not at 2 weeks, suggesting that cerebrovascular impairments precede cognitive dysfunction. In line with the endothelial deficits, carotid stiffness led to increased blood-brain barrier permeability in the hippocampus ($P<0.01$). This region also exhibited reductions in vessel number containing collagen IV ($P<0.01$), as did the somatosensory cortex ($P<0.05$). No evidence of cerebral microhemorrhages was present. Carotid stiffness did not affect the production of mouse amyloid-β (Aβ) or tau phosphorylation, although it led to a modest increase in the Aβ40/Aβ42 ratio in frontal cortex ($P<0.01$).

***Conclusions*—**These findings suggest that carotid stiffness alters brain microcirculation and increases blood-brain barrier permeability associated with cognitive impairments. Therefore, arterial stiffness should be considered a relevant target to protect the brain and prevent cognitive dysfunctions. **(*J Am Heart Assoc*. 2019;8:e011630. DOI: 10.1161/JAHA.118.011630.)**

Key Words: arterial stiffness • blood-brain barrier • carotid calcification • cerebral blood flow • cognitive impairment

Epidemiologic studies have associated large-artery stiffness to cognitive decline and dementia, such as Alzheimer disease.[1–5] Stiffness in large elastic arteries refers to the reduced capability of these vessels to buffer the pulsatile blood flow that arises with each heart contraction (also known as Windkessel effect) and comprises several mechanisms affecting arterial flexibility, such as calcification, endothelial dysfunction, fibrosis, atherosclerosis, and vascular remodeling.

Despite the evidence associating arterial stiffness with cognitive decline, the precise mechanisms of brain dysfunction induced by arterial stiffness remain largely unknown. This is partly because, in humans, arterial stiffness is accompanied by other conditions that can affect the brain and that also arise during aging (eg, hypertension, diabetes mellitus), making it difficult to dissect the contribution of each individual parameter.

To examine this, we previously developed a new murine model of arterial stiffness based on carotid calcification.[6] The advantage of this model over previous ones is that it is the only model in which the elements making the arteries stiffer do not affect the brain in parallel. Specifically, the animals do

From the Départements de Pharmacologie et Physiologie (G.M., D.V., J.Y., H.G.), Neurosciences (M.F.I.), and Nutrition (G.F.) and Groupe de Recherche sur le Système Nerveux Central (M.F.I., H.G.), Université de Montréal, Québec, Canada; Département de Psychiatrie et Neurosciences, Université Laval, Québec, Québec, Canada (M.G., F.R.P., E.P.); Centre de Recherche du CHU de Québec, Québec, Québec, Canada (E.P.); Centre de Recherche de l'Institut de Cardiologie de Montréal, Montréal, Québec, Canada (G.F.); Centre de Recherche de l'Institut Universitaire de Gériatrie de Montréal, Montréal, Québec, Canada (H.G.).

Accompanying Data S1, Tables S1 and S2, and Figures S1 through S3 are available at https://www.ahajournals.org/doi/suppl/10.1161/JAHA.118.011630

*Mr Muhire and Dr Iulita contributed equally to this work.

Correspondence to: Hélène Girouard, PhD, Département de Pharmacologie et Physiologie, Université de Montréal, Pavillon Roger-Gaudry, 2900 Édouard-Montpetit, Montréal, Québec, Canada H3T 1J4. E-mail: helene.girouard@umontreal.ca

Received November 30, 2018; accepted April 15, 2019.

Clinical Perspective

What Is New?

- This study is the first demonstration of a direct cause-effect relationship between arterial stiffness and cerebrovascular alterations.

What Are the Clinical Implications?

- The knowledge that peripheral arterial stiffness alters cerebral blood flow regulation and the integrity of the cerebral vasculature suggests that targeting arterial stiffness could protect the brain of the elderly and hypertensive patients.

not develop increases in systolic blood pressure or narrowing of the carotid radius, which can themselves result in brain damage independently of stiffness. Mice with carotid calcification develop typical features of arterial stiffness such as decreased arterial compliance and distensibility, increased intima-media thickness, and elastin fragmentation,[6] with a beta index comparable to that of a 75 years-old human.[7]

Besides developing increased carotid stiffness, mice with carotid calcification exhibit increased blood flow pulsatility in large and medium-sized cerebral vessels,[6] which could potentially compromise the cerebral microcirculation and impact cognition. Whether arterial stiffness independently of other factors is sufficient to affect higher brain functions, such as learning and memory, is unclear. Likewise, whether disruption of cerebral blood flow (CBF) regulation precedes the negative effects of arterial stiffness on brain function has not been examined.

This is important considering that the vertebrate brain is highly vascularized, and continued perfusion is central to meeting its high metabolic demand. Thus, the brain relies on 3 major regulatory mechanisms: (1) autoregulation, (2) neurovascular coupling, and (3) endothelial regulation.[8] Cerebrovascular autoregulation is the process by which CBF remains constant within a certain range of arterial pressures (60–120 mmHg).[9] This is an important regulatory control given that blood pressure exhibits circadian variations (eg, during sleep) and may also vary during daily activities (eg, exercise), which could potentially impact on cerebral perfusion. Neurovascular coupling is the dynamic link that combines the increase in neural activity to a vasodilatory response.[10] Impairments in neurovascular coupling affect the delivery of nutrients (oxygen, glucose) to active brain cells and slow the clearance of brain metabolites, including potentially toxic ones, which could lead to brain dysfunction. Finally, cerebral endothelial cells are vital for the regulation of vascular tone[11] and for the integrity of the blood-brain barrier, whose function is key to the maintenance of brain homeostasis.[12] Neurovascular alterations, at the level of the blood-brain barrier or attributable to reduced cerebral perfusion, have been identified as key mechanisms for the reduced clearance, and hence buildup, of brain amyloid-β (Aβ) peptides in Alzheimer disease.[13,14]

To provide a deeper understanding of the mechanisms by which arterial stiffness affects the brain, we performed an in vivo study in mice to examine whether carotid stiffness is sufficient to impair cognition, resting CBF, and regulated cerebrovascular responses. We further characterized potential mechanisms that could contribute to brain degeneration caused by carotid stiffness, by examining the integrity of the blood-brain barrier, cerebral microhemorrhages, and cerebrovascular density as well as Aβ and tau pathologies, the 2 main hallmarks of Alzheimer disease. A better understanding of the temporal development of these alterations is crucial for the identification of relevant targets to protect the brain in vulnerable populations with high arterial stiffness, such as the elderly and hypertensive individuals.

Methods

This article adheres to the Transparency and Openness Promotion guidelines. All data, methods, and materials used to conduct the research are available from the corresponding author upon reasonable request.

Animals

All procedures were approved beforehand by the Animal Care Committee of Université de Montréal and were performed in accordance with the guidelines of the Canadian Council on Animal Care and the Animal Research Reporting of In Vivo Experiments guidelines. Ten- to 12-week-old C57BL/6 male mice (Charles River Laboratories, Saint-Constant, Canada) were housed individually in a temperature-controlled room and maintained on a 12-hour light/12-hour dark cycle with ad libitum access to water and a standard rodent diet (Envigo #2018 Teklad global 18% protein rodent diet). Examinations of sex differences on the effects of carotid stiffness on brain function are part of a separate study. Following acclimation, mice were randomly assigned to 2 groups receiving either a periarterial application of NaCl (control group) or $CaCl_2$ (carotid stiffness group). Based on previous experiments on analysis of CBF and cognition, it was determined that a minimum of n=6 mice per group would be required. For all other exploratory analyses, a minimum of n=4 mice per group were used. For each experiment, the number of animals is specified in the text and figure legends. Exclusion criteria are detailed in the corresponding experimental sections. Experimental analyses were done on the right side of the brain

(corresponding to the side of the calcified carotid) and compared with a noncalcified control group rather than to the left side in calcified mice, given that we have previously observed increases in blood flow pulsatility in this hemisphere, although to a smaller extent than that of the right side.[6]

Carotid Calcification

Animals were handled during the 2 days preceding the surgery. Mice were anesthetized with a mixture of ketamine/xylazine (90 mg/kg; 6 mg/kg; CDMV, Saint-Hyacinthe, Canada) and the right common carotid artery was carefully isolated and a small piece of sterile parafilm was slid underneath. A sterile gauze (5×5 mm) soaked in 0.3 mol/L $CaCl_2$ (Sigma-Aldrich, Oakville, Canada) was applied on the carotid artery for 20 minutes. The gauze and parafilm were then removed and the incision sutured. Control animals received a sterile compress soaked in 0.9% NaCl in identical conditions. Carprofen (Rimadyl, 5 mg/kg; CDMV, Saint-Hyacinthe, Canada) was injected subcutaneously as the primary anti-inflammatory analgesic after the surgery and was administered every 24 hours during 2 consecutive days. The day of the surgery, mice also received bupivacaine hydrochloride (Marcaine, 4 mg/kg subcutaneous injection; CDMV, Saint-Hyacinthe, Canada) at the site of the incision, and trimethoprim sulfadiazine (Tribrissen, 30 mg/kg subcutaneous injection; CDMV, Saint-Hyacinthe, Canada) every 24 hours for 3 days to prevent infections. The weight of the animals was monitored weekly after the surgery to verify good recovery. There were no significant mortality (4%) events resulting from the surgery in any of the groups. Upon euthanasia, carotids were dissected and calcification was confirmed with the Von Kossa stain in 4 μM paraffinized tissue sections (performed at the Institute for Research in Immunology and Cancer, Université de Montréal), to visualize calcium deposits.[15] Images were acquired with a Leitz Diaplan microscope equipped with an Olympus DP21 camera (Wild Leitz GmbH, Germany).

Blood Pressure

Systolic blood pressure was monitored by noninvasive tail-cuff plethysmography (Kent Scientific Corp, Torrington, CT) 2 days before the periarterial application of $CaCl_2$ or NaCl (day 0) and weekly for 3 weeks, as detailed in Data S1.

Morris Water Maze

Spatial learning and memory was assessed at 2 and 3 weeks following the periarterial application of NaCl or $CaCl_2$. The testing arena consisted of a circular pool (160 cm in diameter) filled with water made opaque with skim milk powder. The temperature of the water was kept at 18 to 19°C. The pool was divided into 4 virtual quadrants referred to as north, south, east, and west. A clear plexiglass escape platform (10 cm diameter) was placed 1.5 cm beneath the surface in the southwest quadrant. To examine spatial learning, escape latencies were measured during a period of 5 training days (D1–D5), during which mice were allowed three 60 seconds trials per day to find the escape platform. Each trial was 20 minutes apart. Mice were released from a different quadrant each time. An average of the time spent to locate the platform (latency) during the 3 trials was calculated per day per mouse. Latencies to locate the platform were plotted for each training day. The average latency across the entire training and the area under the learning curve were also calculated to compare learning performance.

A probe test (to assess the memory recall) and a cue test (to assess the visual accuracy) were performed on day 6. For the probe test, the platform was removed, and two 30-second trials, 1 hour apart, were conducted to assess time spent in the target quadrant (the place where the platform was originally located), the number of target crossings, and the latency to reach the target quadrant. Swimming speed was determined as a measure of locomotor activity and to ensure that latencies were not confounded by physical impairments. During the cue test, some water was removed so that the escape platform could be visible. Animals with visual impairments were excluded from the analysis. Data were acquired with the Smart Video Tracking Software (Smart version 3.0.01, Panlab Havard apparatus, USA), connected to an overhead camera. The experimenter was blinded to the treatment assignment (NaCl or $CaCl_2$).

Autoradiography

Resting CBF was measured 2 weeks after the periarterial application of NaCl or $CaCl_2$ in awake mice by quantitative autoradiography, using [^{14}C]IAP (Iodoantipirine 4-N-Methyl-^{14}C; Perkin Elmer, Woodbridge, Canada) as a diffusible tracer. The protocol was adapted from Joutel and colleagues[16] and is detailed in Data S1. Brain sections containing the dorsal hippocampus (from Bregma −1.82 to −2.18 mm) were used for analysis in the following regions: visual and somatosensory cortices (VSCx), perirhinal and entorhinal cortices (PECx), cornu ammonis area 1 (CA1), cornu ammonis area 2-3 (CA2-3), dentate gyrus (DG), thalamic nuclei (THA), and corpus callosum (CC). Four brain sections per animal were examined, and data from the right hemisphere (corresponding to the side of the calcified carotid) were used for analysis.

In Vivo Laser Doppler Flowmetry

Cerebrovascular autoregulation as well as CBF responses to whisker stimulation as well as to endothelium-dependent and

-independent vasodilators were examined on the right somatosensory cortex, 2 weeks after the periarterial application of NaCl or $CaCl_2$. Details on the surgical procedures are available in Data S1.

Autoregulation was investigated based on the protocol of Niwa and colleagues.[17] Hypotension was induced by controlled exsanguination to reduce blood pressure every 10 mmHg. In a separate group of mice, mean arterial blood pressure was elevated every 10 mmHg up to 160 mmHg by infusion of 20 to 30 μg/mL phenylephrine (Sigma-Aldrich, Oakville, Canada) via the femoral artery. Given that mice with carotid calcification, but not controls, exhibited breathing distress episodes at the highest pressures (140–160 mmHg), results are presented up to 130 mmHg only. Blood pressure was allowed to stabilize for 5 minutes following each manipulation, after which CBF perfusion units were determined. Results are expressed as percent change with respect to CBF values prior to the change in blood pressure. Neurovascular coupling was examined with 3 whisker stimulations (1 minute duration, spaced every 3 minutes) on the contralateral side from the probe location. Endothelium-dependent responses were measured during the superfusion of acetylcholine 10 μmol/L (Sigma-Aldrich, Oakville, Canada) for 5 minutes followed by a 15 minutes artificial cerebrospinal fluid superfusion to restore CBF responses to basal levels. Endothelium-independent responses were examined with the superfusion of sodium nitroprussiate (SNP) 50 μmol/L (Sigma-Aldrich, Oakville, Canada), a nitric oxide donor. Relative changes in CBF (percent increase in CBF after stimulation compared with baseline) were analyzed with LabChart6 Pro software (version 6.1.3, AD Instruments, USA). Experimental analyses were compared with a noncalcified control group rather than to the contralateral side in calcified mice, given that we have previously observed small significant increases in blood flow pulsatility in this hemisphere.[6]

Tissue Preparation for Histology and Immunostaining

At 3 weeks after surgery, mice were anesthetized with sodium pentobarbital (100 mg/kg body weight; CDMV, Saint-Hyacinthe, Canada) and perfused with 40 mL of phosphate-buffered saline (PBS), pH 7.4. The brains were removed and immersed in cold 4% paraformaldehyde (Bioshop, Burlington, Canada) for 24 hours and then transferred to 30% sucrose for 24 hours. Brains were stored at −20°C in cryoprotectant solution (37.5% v/v ethylene glycol, 37.5% w/w sucrose, in PBS pH 7.4) until sectioning. The right side of the brain was identified, and 40 μM coronal sections were cut with a vibratome (Leica VT 1000S, Leica Biosystems, Germany).

Collagen IV Immunostaining

Collagen IV immunostaining was done adapting the protocol from Franciosi and colleagues[18] and examined at 3 weeks after surgery. Briefly, brain sections were washed 4 times in PBS at room temperature followed by 1 wash with ddH_2O preheated at 37°C. Antigen retrieval was done with pepsin (1 mg/mL) dissolved in 0.2 N HCl for 10 minutes at 37°C followed by 1 wash with warm PBS (at 27°C) and 3 PBS washes at room temperature. Normal goat serum (5%, dissolved in PBS-Triton 0.1%) was used for blocking for 90 minutes at room temperature. The primary antibody (rabbit anticollagen IV, Millipore, Oakville, Canada #AB756P) was incubated at 1:500 in blocking solution overnight at room temperature. The following day, brain sections were washed once with PBS for 5 minutes and later for 1 hour. Incubation with the secondary antibody (goat antirabbit Alexa Fluor 488 at 1:800, Invitrogen-Thermo Fisher Scientific, Burlington, Canada) was done for 2 hours under agitation at room temperature, in PBS-T (Triton 0.1%) with normal goat serum (5%). Following washes in PBS, sections were mounted, allowed to dry, and then coverslipped.

Z-stacked (1.0 μm) confocal images were acquired with an Olympus laser-scanning microscope (model FV1000MPE). At least 3 brain sections per mouse were imaged from the right primary somatosensory cortex as well as from the hippocampal regions CA1), and DG (from Bregma −1.46 to −1.94 mm).

The percentage of collagen IV-positive area per micrograph was calculated with the ImageJ software (National Institutes of Health, Bethesda, MD), as per published protocols for microvascular density analysis.[19] For vascular area, the background was first subtracted with the despeckle and median filter (1.0 pixel) functions, and after threshold adjustment and skeletonization, the area covered by the skeleton of cerebral vessels was calculated. Because the resorption of collagen IV occurs after endothelial loss, the quantification of collagen IV skeleton is a very good marker of complete capillary loss.[20] To minimize variability due to different batches, results were expressed as fold change with respect to the control group.

Microhemorrhages

Microhemorrages were examined with the Prussian blue staining at 3 weeks after surgery, as detailed in Data S1. The following regions were analyzed: frontal cortex, somatosensory cortex, and the hippocampal regions CA1 and DG.

Sodium Fluorescein Extravasation Assay

Blood-brain barrier permeability was examined by the extent of sodium fluorescein (NaF) extravasation to the brain at 3 weeks after surgery. A solution of 10% NaF (Sigma-Aldrich,

Oakville, Canada) was injected intraperitoneally (100 μL) and allowed to circulate for 30 minutes. Mice were then anesthetized with sodium pentobarbital (100 mg/kg body weight; CDMV, Saint-Hyacinthe, Canada) and perfused with 40 mL of cold PBS, pH 7.4. The right frontal cortex, hippocampus, and rest of the cortex were dissected. All tissues were frozen at −80°C until analysis. Brain tissues were weighted and homogenized in 10X cold PBS, pH 7.4, and centrifuged 15 minutes at 14 000*g* at 4°C. The supernatant was recovered, mixed with an equal amount of 15% trichloroacetic acid (Sigma-Aldrich, Oakville, Canada) and centrifuged 15 minutes at 15 000*g* at 4°C. The resulting supernatant was neutralized with 5 mol/L NaOH (diluted 1:5) and mixed. For all samples (standards and unknowns) 100 μL were used for analysis (in duplicate). Relative fluorescence units (excitation 480 nm, emission 525 nm) were read with a fluorometer (SpectraMax M2, Molecular Devices, Sunnyvale, USA) and data were extracted with the SoftMax Pro software (v5.2, Molecular Devices, Sunnyvale, CA). The amount of NaF in brain was calculated from a standard curve (0–5 μmol/L NaF) and normalized per gram of tissue. Results were expressed as fold change with respect to the control group.

Aβ40 and Aβ42 ELISA

Endogenous mouse Aβ40 and Aβ42 were measured by ELISA (KMB3481 and KMB3441, Life Technologies, Invitrogen-Thermo Fisher Scientific, Burlington, Canada) 3 weeks after surgery, as detailed in Data S1.

Tau Western Blot

Examination of phospho-tau levels was done 3 weeks after surgery, following our published protocol[21] and as detailed in Data S1.

Statistical Analysis

Data are displayed in box-and-whisker plots, where the median is represented by the horizontal line, and the 10th and 90th percentiles extend from the extremes of the box. Empty circles represent points below and above the whiskers. Data are displayed as mean±SD. Data analysis was performed with GraphPad Prism software (version 7.05a, La Jolla, USA). ANOVA for factorial design with repeated measures followed by a Fisher's least significant difference posttest for multiple group comparisons was used for analysis of the behavioral data. In the learning curve analysis, the repeated factor is the measure of latency through different time points (D1–D5) and the treatment as a between-group factor. The area under the learning curve was calculated with the area under the learning curve function. In the cerebral autoregulation analysis, a linear regression has been made in order to compare the slopes of treatment and control before and after the diverging point set at 70 mmHg, 100% change in CBF.

For autoradiography, significance of comparisons was tested with a 2-tailed unpaired Student *t*-test per independent brain region; however, results are presented in a single graph. A 2-tailed unpaired Student *t*-test was used for all other 2-group comparisons. Significance was set at $P<0.05$. Sample size per group is presented with the text and figures.

Results

Arterial stiffness was induced by the application of $CaCl_2$ to the right carotid artery. Carotid calcification was confirmed with the Von Kossa stain, revealing the formation of calcium deposits on the carotid of mice treated with $CaCl_2$ examined 2 and 3 weeks after surgery (Figure S1A, right panels). Calcium deposits were absent in mice exposed to NaCl (Figure S1A, left panels). Carotid calcification did not result in an increase in systolic blood pressure, even at 3 weeks after calcification (Figure S1B).

Carotid Stiffness Impairs Learning and Memory

The mice's cognitive abilities were tested with the Morris water maze. At 2 weeks after surgery, mice subjected to the periarterial application of $CaCl_2$ exhibited a progressive decrease in escape latencies during the training phase, as did control animals (Figure 1A; main effect of time: $F[4, 60]=23.07$; $P<0.0001$; n=8–9). Latencies between the 2 groups did not differ at any day during training; neither did the area under the learning curve (137.2±33.8 NaCl versus 134.1±17.7 $CaCl_2$, data not shown) or the average latency across the 5 days (Figure 1B), indicating absence of learning impairments at this time point.

In contrast, at 3 weeks after surgery, mice with carotid stiffness exhibited initially greater mean escape latencies at day 2 (41.7±14.4 versus 28.3±11.9 seconds, simple main effect $P<0.05$; n=9–13), although with continued training they exhibited escape latencies comparable to control mice during the remaining days (Figure 1C; $F[4, 80]=16.02$; $P<0.0001$; n=9–13). There were no significant differences in the area under the learning curve (108.0±30.8 NaCl versus 125.1±41.1 $CaCl_2$, data not shown) or in the overall average latencies through the entire training (Figure 1D); however, the median overall latency for mice with carotid stiffness was 33.8 seconds, while the median latency for controls was 24.1 seconds.

Following the learning period, memory recall was measured with a probe test 24 hours later. Mice subjected to carotid calcification for 2 weeks did not manifest differences

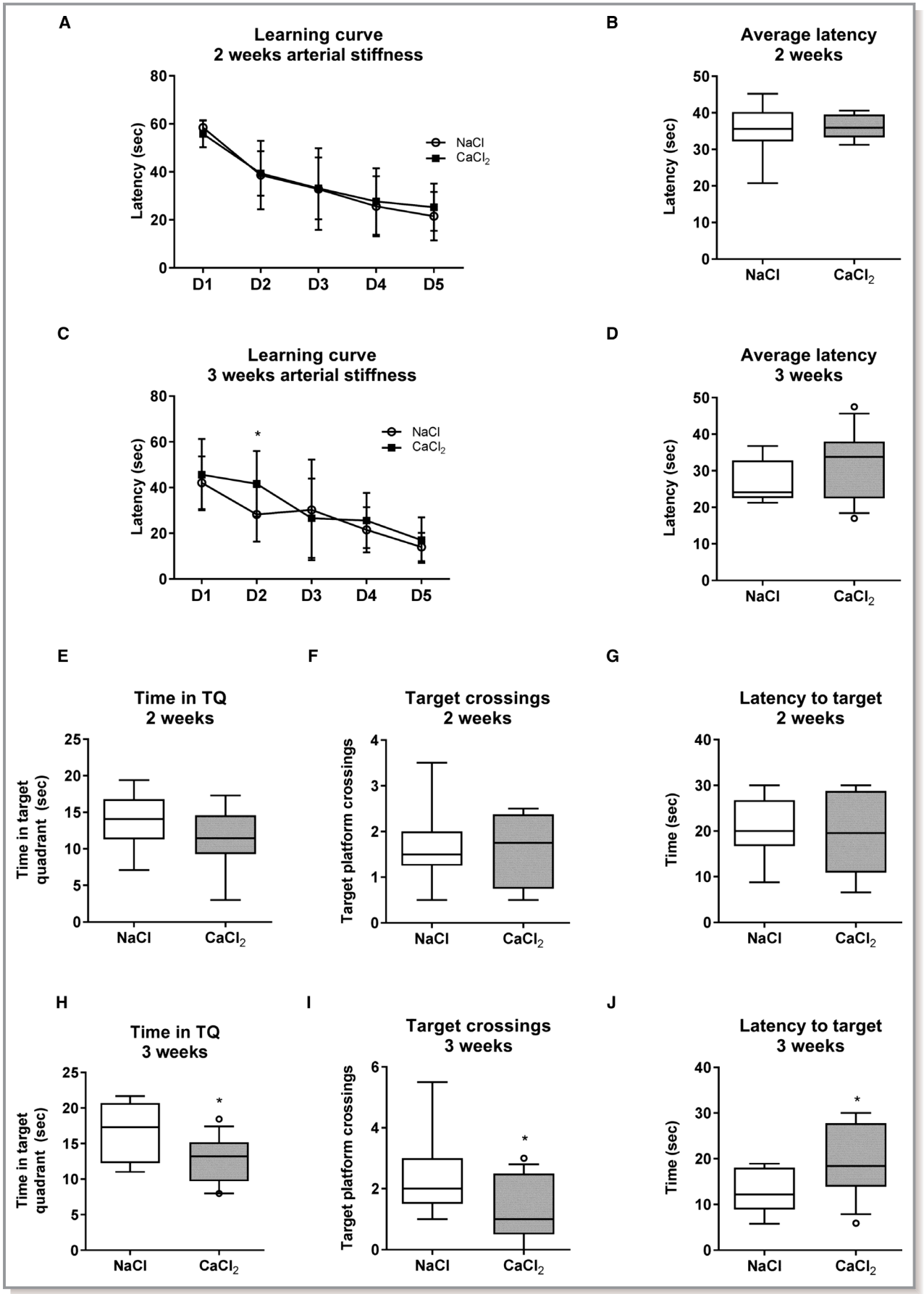
A
Learning curve
2 weeks arterial stiffness
Latency (sec)
NaCl
CaCl2
D1
D2
D3
D4
D5
B
Average latency
2 weeks
Latency (sec)
NaCl
CaCl2
C
Learning curve
3 weeks arterial stiffness
Latency (sec)
*
NaCl
CaCl2
D1
D2
D3
D4
D5
D
Average latency
3 weeks
Latency (sec)
NaCl
CaCl2
E
Time in TQ
2 weeks
Time in target quadrant (sec)
NaCl
CaCl2
F
Target crossings
2 weeks
Target platform crossings
NaCl
CaCl2
G
Latency to target
2 weeks
Time (sec)
NaCl
CaCl2
H
Time in TQ
3 weeks
Time in target quadrant (sec)
*
NaCl
CaCl2
I
Target crossings
3 weeks
Target platform crossings
*
NaCl
CaCl2
J
Latency to target
3 weeks
Time (sec)
*
NaCl
CaCl2

Figure 1. Effect of carotid calcification on spatial learning and memory. Cognitive abilities were examined with the Morris Water Maze test (2 and 3 weeks after application of $CaCl_2$ or NaCl) (**A** and **C**). The test consisted of 5 training days (D1–D5) during which mice were allowed three 60 seconds trials per day to find the escape platform. Each trial was 20 minutes apart. The area under the learning curve (AUC) and the average latency across the training (**B** and **D**) were calculated to compare learning performance. Graphs represent mean±SD. Data are displayed in box-and-whisker plots, where the median is represented by the horizontal line, and the 10th and 90th percentiles extend from the extremes of the box. For the probe test (day 6), the platform was removed and animals were given two 30 seconds trials separated 1 hour apart, to assess (**E** and **H**) time spent in the target quadrant (the place where the platform was originally located), (**F** and **I**) number of target crossings and (**G** and **J**) latency to reach the target zone. Data were analyzed with ANOVA for factorial design with repeated measures followed by a Fisher's LSD posttest for multiple group comparisons for the learning curves; unpaired Student *t*-test was used for all other 2-group comparisons; n=8 to 9 mice/group (2 weeks) and n=9 to 13 mice/group (3 weeks). **P*<0.05; TQ indicates target quadrant.

in the time spent in the target quadrant (Figure 1E), in the target crossings (Figure 1F), or in the latency to reach the target quadrant (Figure 1G), indicating absence of memory impairments at this time point. Instead, at 3 weeks after surgery, mice with carotid calcification spent significantly less time in the target quadrant compared with controls (Figure 1H; *P*<0.05; n=9–13). In line with these results, mice with carotid stiffness also performed significantly fewer target crossings (Figure 1I; *P*<0.05, n=9–13) and showed increased time to reach the target zone (Figure 1J; *P*<0.05; n=9–13). Swimming speed was comparable between the 2 groups at both time points (Figure S2).

Carotid Stiffness Leads to Diminished Resting CBF

At 2 weeks after calcification, when cognitive deficits were not yet present, resting CBF was assessed by quantitative

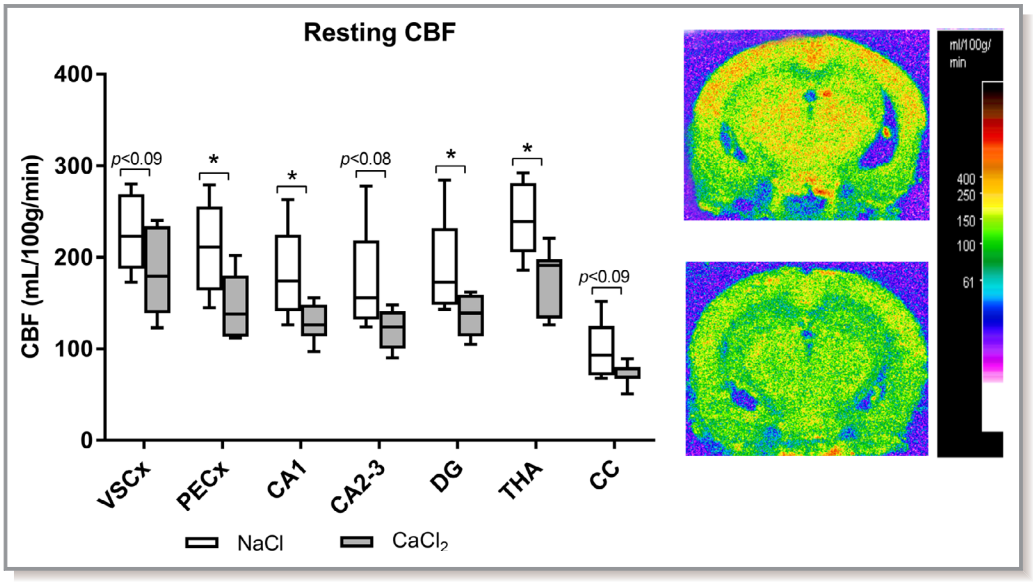

Figure 2. Effect of carotid calcification on resting cerebral blood flow (CBF). Resting CBF was measured by autoradiography using [^{14}C]iodoantipyrine as a diffusible tracer in awake mice, 2 weeks after application of $CaCl_2$ or NaCl. CBF was quantified in the following regions from the right hemisphere: visual and somatosensory cortices (VSCx), perirhinal and entorhinal cortices (PECx), cornu ammonis area 1 (CA1), cornu ammonis area 2-3 (CA2-3), dentate gyrus (DG), thalamus (THA), and corpus callosum (CC). Data are displayed in box-and-whisker plots, where the median is represented by the horizontal line and the 10th and 90th percentiles extend from the extremes of the box. **P*<0.05; unpaired Student *t*-test per independent brain region (results presented in a single graph); n=5 to 7 mice/group. CBF is expressed as mL/100 g/min. Representative blood flow autoradiograms for control (upper panel) and $CaCl_2$ mice (lower panel) are shown with a color scale.

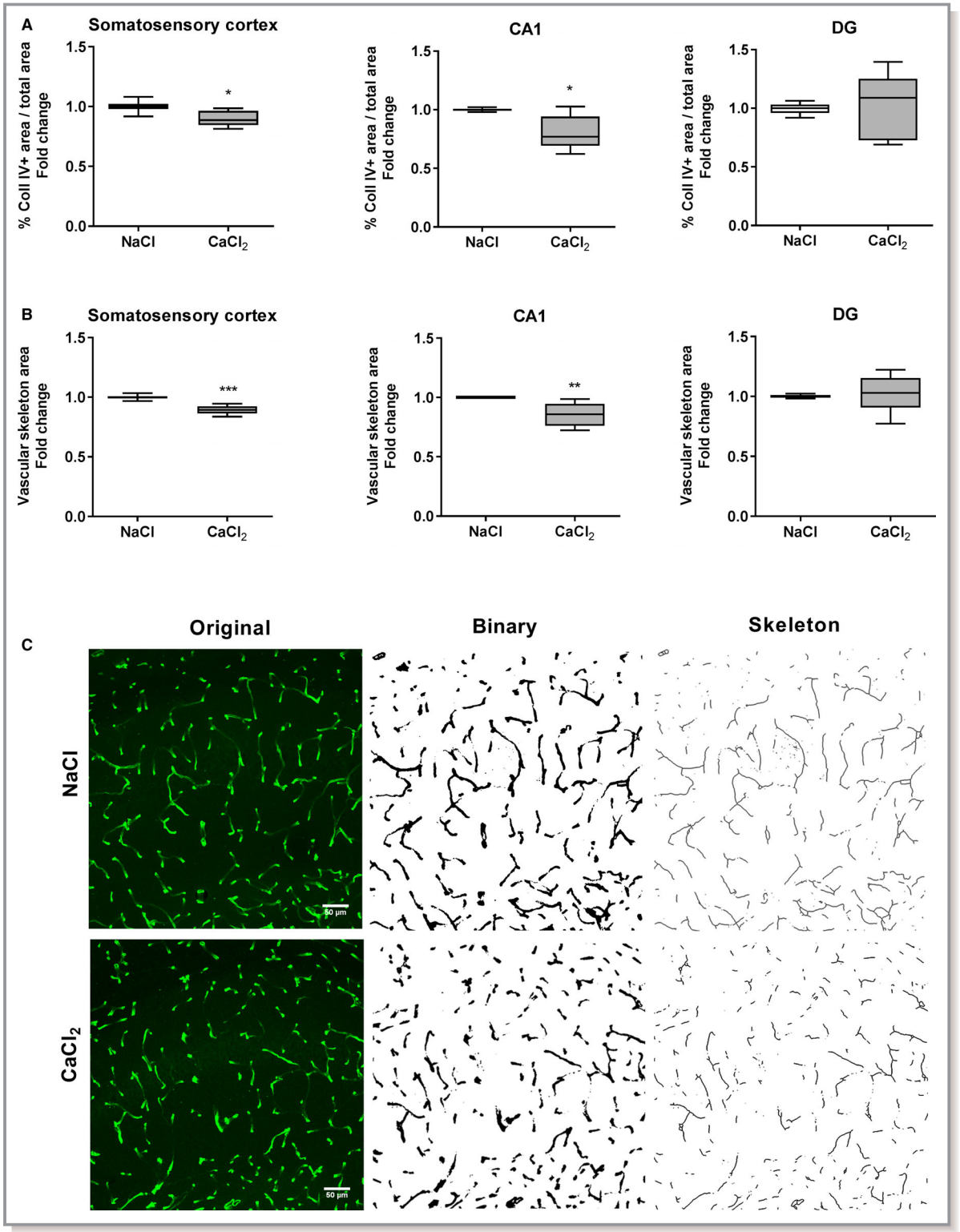

Figure 3. Effect of carotid calcification on number of cerebral vessel containing collagen type IV. Semiquantitative analysis of microvessel number per field by examination of (**A**) collagen IV–positive area percentage and (**B**) vascular skeleton area in the somatosensory cortex and hippocampus (cornu ammonis area 1 [CA1] and dentate gyrus [DG]) from the right hemisphere. Data are displayed in box-and-whisker plots, where the median is represented by the horizontal line, and the 10th and 90th percentiles extend from the extremes of the box. **P*<0.05, ***P*<0.01, ****P*<0.0001; unpaired Student *t*-test, n=5 to 6 mice/group. **C**, Representative micrographs of collagen IV immunostaining, binary transformation, and skeletonization for CA1 are shown. Scale bar=50 µm. Analysis was done 3 weeks after surgery.

autoradiography. Mice with carotid calcification exhibited decreases in resting CBF in several brain regions, including gray and white matter (Figure 2; n=5–7 mice/group). Specifically, carotid calcification led to significant reductions in resting CBF (mean range, 28%–30% decrease) in the perirhinal/entorhinal region ($P<0.05$), in CA1 ($P<0.05$), DG ($P<0.05$), and thalamus ($P<0.05$), with a trend in CA2-3 ($P=0.0768$) and in the VSCx region ($P=0.0896$). Likewise, there was a trend for a decrease in resting CBF in the white matter, measured in the corpus callosum (mean 26% decrease; $P=0.0895$).

Carotid Stiffness Leads to a Diminished Number of Cerebral Vessels Containing Collagen IV

To evaluate whether the decrease in resting CBF was caused by a diminished microvascular density, we assessed whether carotid stiffness would be sufficient to affect the cerebral microvasculature. Analysis of collagen IV immunostaining (Figure 3A) revealed a small but significant reduction in cerebral vessels in the somatosensory cortex of mice subjected to carotid calcification (≈10% decrease; $P<0.05$;

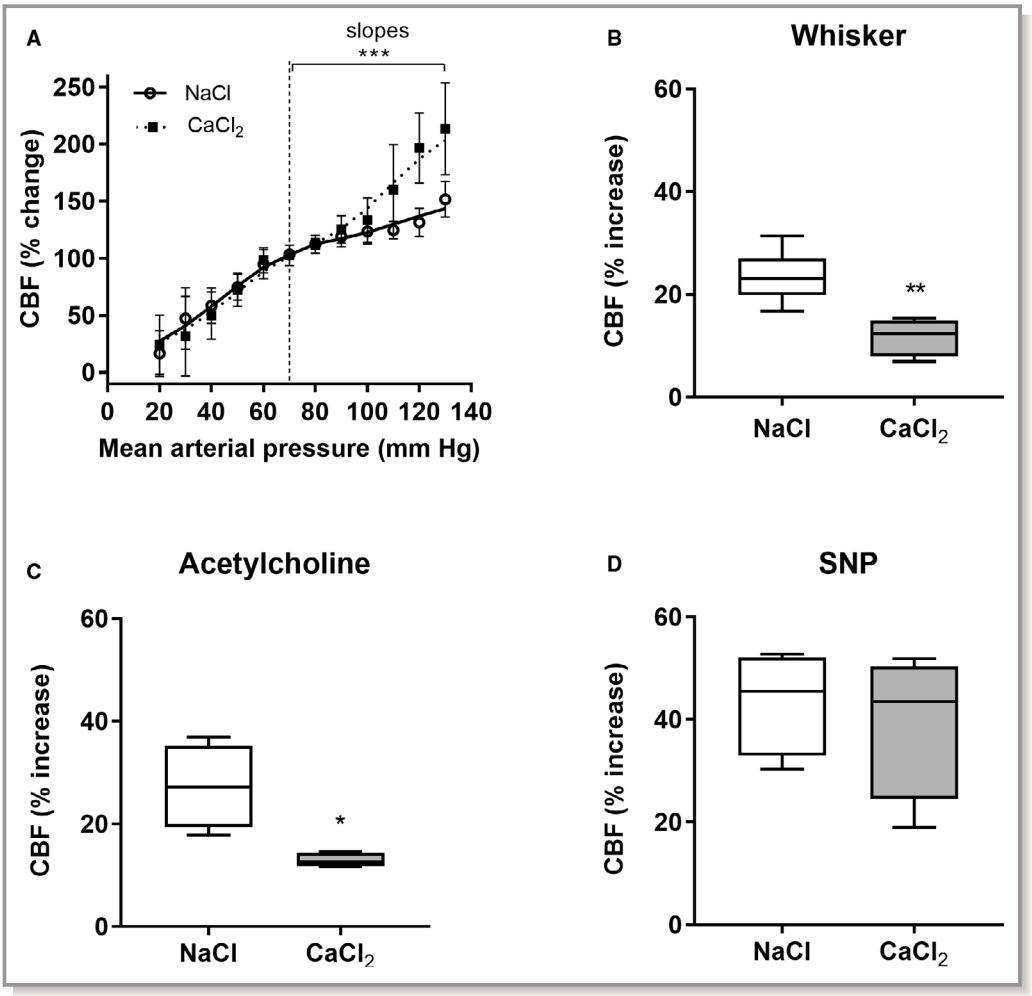

Figure 4. Effect of carotid calcification on cerebrovascular responses. **A**, Analysis of cerebral autoregulation depicting relationship between mean arterial pressure and cerebral blood flow (CBF). Graph represents mean±SD. Data are displayed in box-and-whisker plots, where the median is represented by the horizontal line, and the 10th and 90th percentiles extend from the extremes of the box. ***$P<0.001$, linear regression of slopes between 70 and 130 mmHg was used; n=5 to 9 mice/group. CBF responses to whisker stimulation (**B**), to the endothelium-dependent vasodilator, acetylcholine (**C**), and to the endothelium-independent vasodilator, sodium nitroprussiate (SNP; **D**) were evaluated. Graphs depict the percentage increase in CBF following the stimulation with respect to its initial value. *$P<0.05$; **$P<0.01$; unpaired Student *t*-test; n=4 to 6 mice/group. CBF was measured on the right somatosensory cortex by laser Doppler flowmetry 2 weeks after application of $CaCl_2$ or NaCl.

n=6/group) and a more prominent reduction in the CA1 region of the hippocampus (≈19% decrease; $P<0.05$; n=5–6/group). No differences were detected in the DG.

Analysis of the vascular skeleton area followed a similar pattern in mice with carotid stiffness (Figure 3B), with small but significant reductions in skeleton area in the somatosensory cortex (≈11% decrease; $P=0.0001$; n=6/group) and greater reductions in CA1 (≈15% decrease; $P<0.01$; n=5–6/group). No differences were detected in the DG. The measures of skeleton area and collagen IV density correlated. Spearman analysis revealed positive associations both in the somatosensory cortex ($r=0.5654$; $P=0.0582$) and in CA1 ($r=0.6989$; $P<0.05$).

Carotid Stiffness Impairs Cerebral Autoregulation, Neurovascular Coupling, and CBF Responses to Endothelial Stimulation

To further investigate the mechanisms of CBF damage due to arterial stiffness, we examined whether carotid calcification affected regulated cerebrovascular responses at the same time point when resting CBF was found impaired (2 weeks after calcification).

While control animals exhibited small variations in CBF within a certain range of arterial pressures (60–120 mmHg), suggesting that autoregulation was operating, these fluctuations were increased in mice with carotid calcification at the highest pressures, significantly differing from control mice (Figure 4A; $F[1, 54]=26.39$; $P<0.001$; n=5–9). The lower limit of autoregulation was not disrupted in mice with carotid stiffness.

Mice subjected to the periarterial application of $CaCl_2$ further exhibited attenuated CBF responses produced by neuronal activity (whisker stimulation) compared with control mice (Figure 4B; NaCl mean 23.5% versus $CaCl_2$ 11.8%; $P<0.01$; n=4–6 mice/group). The loss of autoregulation and impairments in neurovascular coupling in mice with carotid stiffness were also accompanied by attenuated increases in CBF produced by the application of the endothelium-dependent vasodilator, acetylcholine (Figure 4C; NaCl mean 27.2% versus $CaCl_2$ 12.9%; $P<0.05$; n=4 mice/group). In contrast, there were no differences in CBF responses to the nitric oxide donor, sodium nitroprussiate (Figure 4D; n=4 mice/group). Physiological parameters comprising blood pH, pO_2, pCO_2, mean arterial pressure, and CBF at baseline (before the stimulation) were comparable between control and mice with carotid stiffness (Table S1).

Effect of Carotid Stiffness on Cerebral Microhemorrhages

Considering the previously reported increases in the pulsatility of cerebral vessels in this model[6] and impaired autoregulation, cerebral microhemorrhages were examined 3 weeks after calcification, when cognitive deficits were present. Histochemical analysis with the Prussian blue reaction did not reveal the presence of iron deposits, neither in the frontal or somatosensory cortex nor in the hippocampus of mice subjected to arterial stiffness (Figure S3).

Carotid Stiffness Increases Blood-Brain Barrier Permeability in the Hippocampus

Given the deficits in cerebral endothelial responses, we next tested the hypothesis that the permeability of the blood-brain barrier would be affected as a consequence of carotid

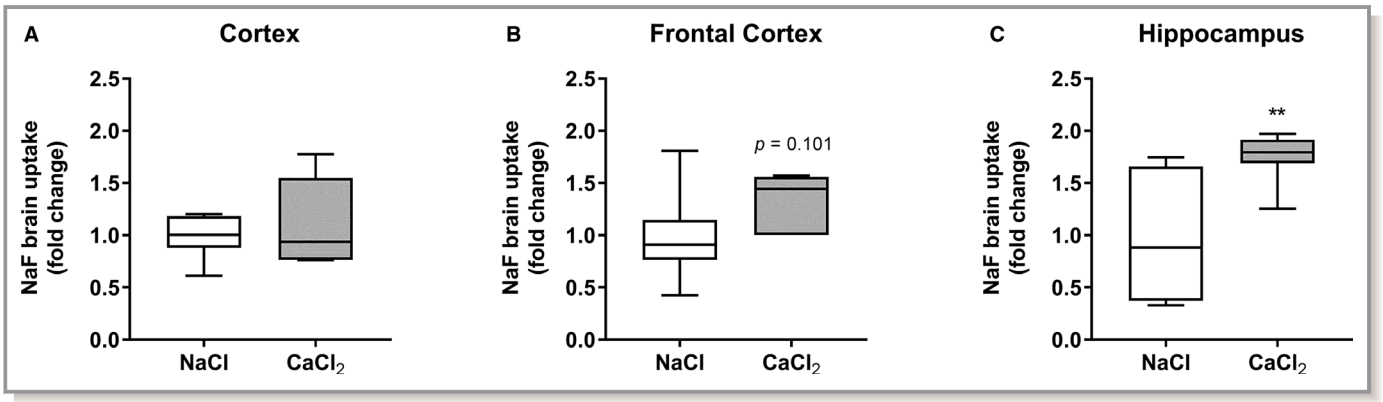

Figure 5. Effect of carotid calcification on blood-brain barrier permeability. Permeability of the blood-brain barrier was examined by sodium fluorescein (NaF) extravasation in specific brain regions cortex (**A**), frontal cortex (**B**) and hippocampus (**C**) from the right hemisphere 3 weeks after application of $CaCl_2$ or NaCl. The amount of NaF in each region was calculated from a standard curve (0–5 μmol/L NaF) and normalized per gram of tissue. Results are expressed as fold change by normalizing values to the average of the control group. Data are displayed in box-and-whisker plots, where the median is represented by the horizontal line, and the 10th and 90th percentiles extend from the extremes of the box. $**P<0.01$; unpaired Student *t*-test, n=7 mice/group.

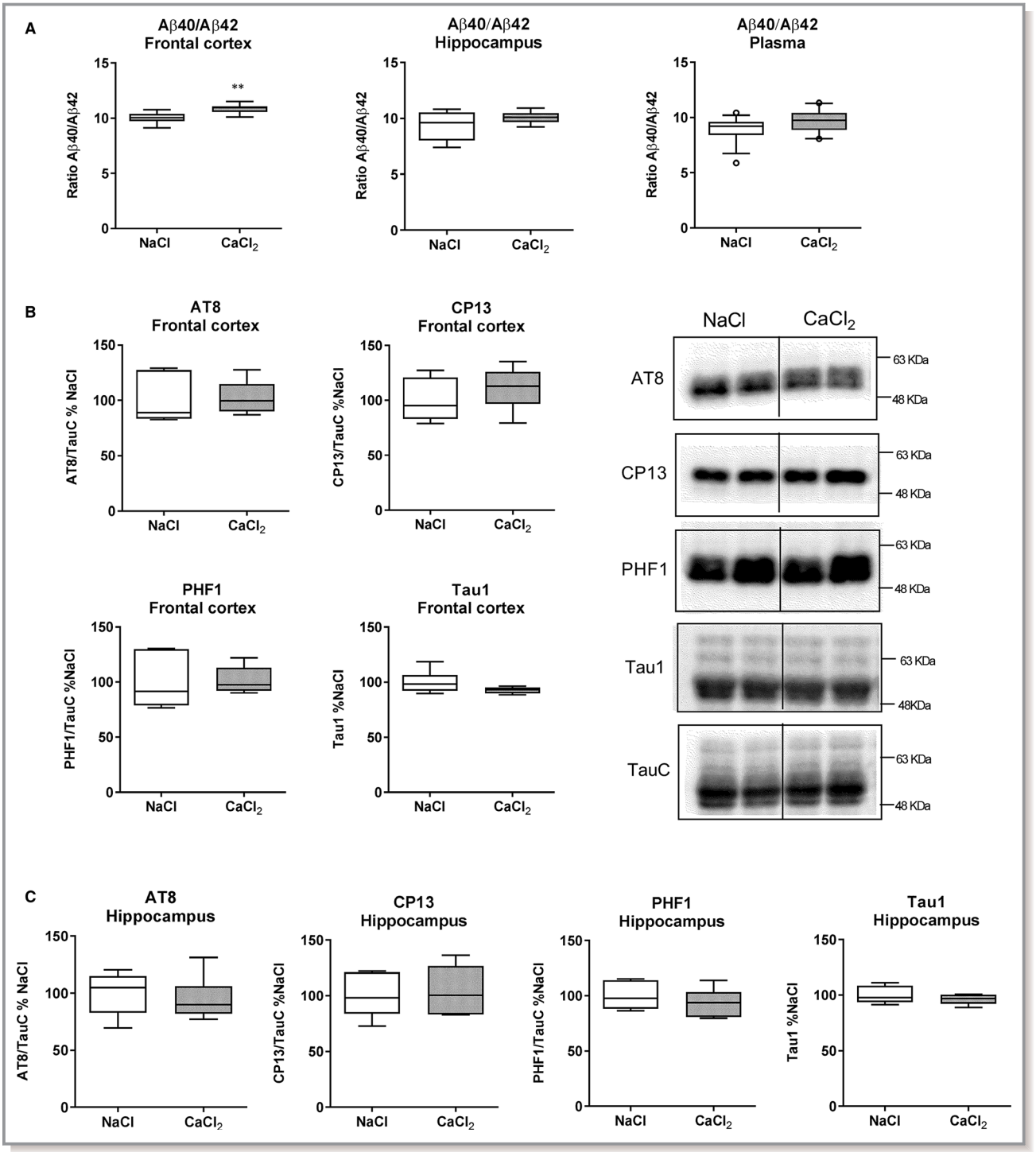

Figure 6. Effect of carotid calcification on amyloid-β (Aβ) and tau hyperphosphorylation. **A**, The Aβ40/Aβ42 ratio was calculated from Aβ concentrations determined by ELISA in the frontal cortex and hippocampal tissue as well as in plasma. Expression of phosphorylated tau (AT8, CP13 and PHF1) and dephosphorylated tau (Tau1) in frontal cortex (**B**) and hippocampus (**C**) examined by western blotting. Representative immunoblots are shown. Data are displayed in box-and-whisker plots, where the median is represented by the horizontal line and th,e 10th and 90th percentiles extend from the extremes of the box. $^{**}P<0.01$; unpaired Student *t*-test, n=6 to 7 mice/group in frontal cortex and hippocampus, n=10 to 15 mice/group in plasma. Analysis was done 3 weeks after surgery on frozen tissue from the right hemisphere.

stiffness. The increase in sodium fluorescein brain uptake in mice subjected to carotid calcification was region specific (Figure 5). While there were no differences in sodium fluorescein uptake in the brain cortex (Figure 5A; n=7/group), a trend suggesting incipient increase in blood-brain barrier permeability was observed in the frontal cortex (Figure 5B; mean 1.3 fold change; P=0.1013; n=7/group). Notably, the hippocampus exhibited the most significant differences in sodium fluorescein uptake (Figure 5C; mean 1.7-fold; P<0.01; n=7/group), suggesting that this region was highly vulnerable to blood-brain barrier damage.

Effect of Carotid Stiffness on Amyloid and Tau Pathology

Given the epidemiologic associations between arterial stiffness and dementia, and the brain vascular damage reported in this study, we questioned whether such changes could have an impact on Aβ buildup and tau hyperphosphorylation, the 2 main pathological hallmarks of Alzheimer disease.

Although the absolute concentrations of brain Aβ peptides did not differ between groups (Table S2), quantitative analysis revealed a modest but significant increase in the ratio Aβ40/42 in the frontal cortex of mice with carotid stiffness (Figure 6A; P<0.01; n=6–7), with a similar trend in the hippocampus, although not significant (Figure 6A; n=6–7). There were also no significant differences in the ratio of circulating Aβ peptides measured in plasma between mice with carotid stiffness and controls (Figure 6A; P=0.1369; n=10–15).

In line with the modest changes in Aβ, there were no significant differences in the expression of phosphorylated tau, examined by the assessment of several phospho tau epitopes in the same brain regions where Aβ was measured (Figure 6B and 6C; n=6/group). There were also no differences in the expression of dephosphorylated tau (Tau1) or total tau levels (TauC), the latter being used for normalization of phospho tau signals.

Discussion

Arterial stiffness, a common condition that arises with aging, is emerging as a strong and independent risk factor for early cognitive impairment and dementia,[22,23] as recently reviewed.[24] Arterial stiffness may contribute to cerebral dysfunction via numerous effects, which until now have been difficult to dissect in human studies attributable to multiple factors that may affect the brain being present in parallel.

In this study, we address this issue by characterizing the impact of carotid stiffness on brain function with a unique murine model based on carotid calcification,[6] specific for this vascular parameter. Our findings indicate that carotid stiffness, independently of aging or increased blood pressure, alters the regulation of CBF and the integrity of the cerebral vasculature, increasing the blood-brain barrier permeability and leading to cognitive deficits.

Mice with carotid calcification exhibited significant impairments in resting CBF and in the mechanisms that regulate cerebrovascular responses, including cerebral autoregulation, neurovascular coupling, and endothelial dilatation. These deficits preceded the manifestation of spatial memory impairments. Resting CBF was found diminished in critical brain regions including the hippocampus and entorhinal cortex, which are highly vulnerable areas important for memory and one of the earliest affected in patients with Alzheimer disease,[25] the most common form of dementia in elderly subjects. The decrease in resting CBF, measured by autoradiography, could be explained at least partly by a decrease in vascular density as determined by analyzing the collagen IV skeleton area. Although autoradiography is an invasive technique, it provides a better resolution than other noninvasive techniques such as magnetic resonance imaging for small brain vessel studies in mice. A decrease in CBF and vascular density may lead to hypoxia-induced neurodegeneration. Interestingly, we previously demonstrated the presence of degenerative neurons as determined by the Fluorojade B method in the subarea of the CA1 region called lacunosum moleculare.[6] In agreement with our study, a disconnect between neuronal function and blood supply, as well as reduced resting CBF, has been reported in Alzheimer patients at early disease stages and associated with cognitive deterioration.[26]

Alterations in cerebral autoregulation have been linked to hypertension, diabetes mellitus, ischemic stroke, and Alzheimer disease.[27–30] To maintain a constant cerebral perfusion, the brain relies on the capacity of cerebral arteries to constrict upon increases in systemic pressure and to dilate when arterial pressure lowers. Our results showing compromised autoregulation in the upper range of arterial pressures would indicate a failure in vasoconstriction of cerebral vessels, which would lead to hyperperfusion and disruption of the blood-brain barrier.[31] Interestingly, in a murine model of atherosclerosis, which exhibits certain similarities to ours in terms of increased carotid stiffness, increased pulsatility in cerebral vessels, and cognitive decline, it was shown that cerebral arteries displayed increases in vascular compliance,[32,33] which would be consistent with a failure in vasoconstriction and disruption of the upper limit of autoregulation. Although we have not directly measured the compliance of cerebral arteries in our model, the disruption of endothelial dilatation seen in our mice with carotid calcification would indicate that this is a likely possibility, considering that cerebral endothelial function may modulate cerebrovascular wall biomechanics.[34]

While other mechanisms may also contribute to impairing cognition, the physiological repercussions of a dysfunctional regulation of CBF are significant considering the brain's high metabolic needs and the fact that even small blood flow reductions can lead to the inhibition of protein synthesis and to neuronal dysfunction.[35] In addition, normal CBF is necessary for the removal of metabolic by-products. Thus, the initial appearance of CBF deficits followed by diminished memory recall in our model would suggest that disruption of CBF regulation is a mechanistic link between arterial stiffness and its effects on cognition. In support, a recent clinical study showed that in the Age, Gene/Environment Susceptibility-Reykjavik cohort, the association between high artery stiffness and low memory function included cerebrovascular factors such as increased cerebrovascular resistance and damage to the white matter.[36]

It is important to note that we have controlled for potential perturbations of physiological parameters that could affect CBF (eg, blood gases, arterial pressure) and that these were found to be comparable between controls and mice with carotid calcification. Further evidence that the CBF deficits detected were not spurious results attributable to nonspecific dysfunction caused during the surgeries is the fact that not all cerebrovascular responses were impaired in our model, as seen by the intact CBF responses to sodium nitroprussiate, which is an endothelium-independent vasodilator.

The absence of detectable microhemorrhages in this model at the young age examined (13–15 weeks) further strengthens the finding that the manifestation of memory deficits is likely related to the dysregulation of CBF and decreased cerebrovascular density. We do not discard the possibility that arterial stiffness could promote the formation of microhemorrhages in humans, as these lesions can be common in older adults (≥60 years)[37] and in very elderly individuals (90+ years).[38] Indeed, microhemorrhages have been associated with increased risk of stroke,[39] disruption of white matter structure,[40] lower cognitive function,[41] and even dementia.[38] Given our finding that mice with carotid calcification tended to exhibit impaired CBF in the corpus callosum, the richest region of white matter fibers within the brain, it would be interesting to examine whether arterial stiffness is sufficient to induce microhemorrhages and white matter dysfunction in older animals. We have not considered this possibility in this study to avoid the added confounder of aging and thus to be able to examine the independent effects of carotid stiffening without additional parameters. Besides the issue of aging, our autoregulation results suggest that arterial stiffness accompanied by hypertension may also lead to microhemorrhages. Because we have not seen increases in blood pressure in mice with carotid calcification even beyond 3 weeks after surgery, this could also in part explain the absence of detectable microhemorrhages at this time point in this model. Thus, to better predict the impact of arterial stiffness on the brain, future studies will have to be conducted in old mice with or without hypertension.

In considering other mechanisms that might damage the brain as a result of arterial stiffness, and in view of the cerebral endothelial dysfunction detected, we examined the blood-brain barrier permeability, which is severely damaged in patients with Alzheimer disease and in elderly individuals, particularly in the hippocampus.[42,43] Indeed, in addition to the negative consequences of a reduced CBF, the passage of cytotoxic molecules through a leaky blood-brain barrier may further affect neuronal integrity. Our results showed a region-specific increase in blood-brain barrier permeability attributable to carotid stiffness, with significant permeability in the hippocampus and a similar trend in the frontal cortex, a region affected in patients with vascular disorders.[44,45] The vulnerability of the hippocampus in this carotid stiffness model can be explained by the previously reported increases in vascular superoxide production and microglia activation in this region,[46] which could damage the cerebral endothelium, the site of the blood-brain barrier. It is also consistent with the observation of impaired spatial memory and the significant reductions in number of cerebral vessels containing collagen type IV also seen in this region.

We expected that the altered cerebrovascular regulation, reduced microvessel density, and the blood-brain barrier compromise would have an impact on Aβ clearance and thus lead to Aβ buildup in the brain. Our results showed a modest increase in the ratio Aβ40/Aβ42 in the frontal cortex, while no significant changes were seen in the hippocampus and plasma. This should not rule out that arterial stiffness could have an impact on Aβ accumulation in humans. First, endogenous murine amyloid peptides lack the aggregation-prone amino acids that are present in human Aβ, and their expression is lower compared with humans.[47,48] One way to reexamine the proposed hypothesis would be to evaluate whether arterial stiffness is capable of exacerbating Aβ pathology in transgenic murine models of human amyloid overproduction. Indeed, studies in humans have reported associations between pulse wave velocity (a clinical measurement of arterial stiffness) and brain Aβ burden in nondemented adults,[49,50] warranting future investigations to better understand this association.

Taken together, our findings suggest that carotid stiffness is sufficient to independently induce deficits in the brain microcirculation and to increase the blood-brain barrier permeability. With a compromise in CBF, the proper delivery of oxygen and nutrients to support neuronal function is disrupted, leading to hippocampal neurodegeneration and cognitive impairments. It should be noted that while these changes seem to appear "early" in this model (2–3 weeks after calcification), it is at this time point that mice with carotid calcification exhibit an

increased beta index comparable to that of a 75 years-old human.[6] At the same time, the rapid cognitive decline in mice may be explained by the lack of brain and cognitive reserve in rodents. In humans, brain and cognitive reserve provides neuroprotection and compensation in Alzheimer disease and dementia, but also in other brain disorders,[51] and can reduce the effect of Alzheimer pathology on cognition.[52] Also, the distance between carotid and cerebral arteries is much shorter in mice than in humans, which reduces the dampening capacity of the murine vasculature and makes their brain more vulnerable. Upon technical development of blood pulsatility measures in human cerebral blood vessels, it will be possible to adjust our model and better understand the threshold of stiffness and blood pulsatility that could impact the brain.

Although our study provides new insights on the mechanisms by which arterial function affects the brain, several questions remain unanswered. For example, if the CBF dysregulation were amenable to therapeutic correction, would this prevent or delay the appearance of memory deficits in a context of cerebral inflammation and damaged blood-brain barrier? When should individuals with arterial stiffness qualify for treatments? Which are the best drugs or targets? Answers to these questions will significantly advance our understanding of the impact of arterial stiffness on brain function and help in the development of new strategies to protect the heart and the brain in aging and hypertension.

Acknowledgments

The authors thank Dr Elvire Vaucher (Professor, Ecole d'optométrie, Université de Montréal, Canada) for help with the autoradiography technique, Dr Donna Wilcock (University of Kentucky, USA) for providing assistance for the setup of the microhemorrhages protocol and mouse brain tissue, and Olivia De Montgolfier from Dr Eric Thorin's laboratory (Institut de Cardiologie de Montréal, Canada) for assistance with collagen IV quantification and helpful discussions. We also thank Dr Peter Davies (The Feinstein Institute for Medical Research, New York) for the generous gift of anti-tau antibodies.

Sources of Funding

This research was supported by funding from the Heart and Stroke Foundation of Canada (Girouard), the Fonds de recherche du Québec-Santé (Girouard: # 33237), the Canadian Foundation for Innovation (Girouard: #20089), the Natural Sciences and Engineering Research Council of Canada (Planel: #354722), and the Canadian Institutes of Health Research (Ferland: #MOP-126170, Planel: #MOP-106423, #PCN-102993, Girouard: #MOP-285902). Muhire acknowledges support for a Bourse de recrutement aux cycles supérieurs from the Faculty of Medicine, Université de Montréal (2014). Iulita would like to acknowledge support from the Herbert H. Jasper Postdoctoral Research Fellowship in Neurosciences (2016–2017) from the Groupe de Recherche sur le Système Nerveux Central (GRSNC), Université de Montréal, and for a Bourse Postdoctorale from the Fonds de recherche du Québec - Santé (2016–2019). Youwakim acknowledges support for a Bourse d'Excellence au Recrutement from the Department of Pharmacology and Physiology and the Faculty of Graduate and Postdoctoral Studies of Université de Montréal (2017–2018). Gratuze and Petry were recipients of a Biomedical Doctoral Award from the Alzheimer Society of Canada (2014–2017 and 2012–2015, respectively).

Disclosures

None.

References

1. Pase MP, Herbert A, Grima NA, Pipingas A, O'Rourke MF. Arterial stiffness as a cause of cognitive decline and dementia: a systematic review and meta-analysis. *Intern Med J*. 2012;42:808–815.
2. Hughes TM, Craft S, Lopez OL. Review of "the potential role of arterial stiffness in the pathogenesis of Alzheimer's disease." *Neurodegener Dis Manag*. 2015;5:121–135.
3. Hanon O, Haulon S, Lenoir H, Seux ML, Rigaud AS, Safar M, Girerd X, Forette F. Relationship between arterial stiffness and cognitive function in elderly subjects with complaints of memory loss. *Stroke*. 2005;36:2193–2197.
4. Meyer ML, Palta P, Tanaka H, Deal JA, Wright J, Knopman DS, Griswold ME, Mosley TH, Heiss G. Association of central arterial stiffness and pressure pulsatility with mild cognitive impairment and dementia: the Atherosclerosis Risk in Communities Study-Neurocognitive Study (ARIC-NCS). *J Alzheimers Dis*. 2017;57:195–204.
5. Pase MP, Beiser A, Himali JJ, Tsao C, Satizabal CL, Vasan RS, Seshadri S, Mitchell GF. Aortic stiffness and the risk of incident mild cognitive impairment and dementia. *Stroke*. 2016;47:2256–2261.
6. Sadekova N, Vallerand D, Guevara E, Lesage F, Girouard H. Carotid calcification in mice: a new model to study the effects of arterial stiffness on the brain. *J Am Heart Assoc*. 2013;2:e000224. DOI: 10.1161/JAHA.113.000224.
7. Jurasic MJ, Josef-Golubic S, Sarac R, Lovrencic-Huzjan A, Demarin V. Beta stiffness—setting age standards. *Acta Clin Croat*. 2009;48:253–258.
8. Toth P, Tarantini S, Csiszar A, Ungvari Z. Functional vascular contributions to cognitive impairment and dementia: mechanisms and consequences of cerebral autoregulatory dysfunction, endothelial impairment, and neurovascular uncoupling in aging. *Am J Physiol Heart Circ Physiol*. 2017;312:H1–H20.
9. Paulson OB, Strandgaard S, Edvinsson L. Cerebral autoregulation. *Cerebrovasc Brain Metab Rev*. 1990;2:161–192.
10. Girouard H, Iadecola C. Neurovascular coupling in the normal brain and in hypertension, stroke, and Alzheimer disease. *J Appl Physiol (1985)*. 2006;100:328–335.
11. Faraci FM, Heistad DD. Regulation of the cerebral circulation: role of endothelium and potassium channels. *Physiol Rev*. 1998;78:53–97.
12. Abbott NJ, Patabendige AA, Dolman DE, Yusof SR, Begley DJ. Structure and function of the blood-brain barrier. *Neurobiol Dis*. 2010;37:13–25.
13. Sagare AP, Bell RD, Zlokovic BV. Neurovascular dysfunction and faulty amyloid beta-peptide clearance in Alzheimer disease. *Cold Spring Harb Perspect Med*. 2012;2:a011452.
14. Mawuenyega KG, Sigurdson W, Ovod V, Munsell L, Kasten T, Morris JC, Yarasheski KE, Bateman RJ. Decreased clearance of CNS beta-amyloid in Alzheimer's disease. *Science*. 2010;330:1774.
15. Rungby J, Kassem M, Eriksen EF, Danscher G. The von Kossa reaction for calcium deposits: silver lactate staining increases sensitivity and reduces background. *Histochem J*. 1993;25:446–451.
16. Joutel A, Monet-Lepretre M, Gosele C, Baron-Menguy C, Hammes A, Schmidt S, Lemaire-Carrette B, Domenga V, Schedl A, Lacombe P, Hubner N. Cerebrovascular dysfunction and microcirculation rarefaction precede white matter lesions in a mouse genetic model of cerebral ischemic small vessel disease. *J Clin Invest*. 2010;120:433–445.

17. Niwa K, Kazama K, Younkin L, Younkin SG, Carlson GA, Iadecola C. Cerebrovascular autoregulation is profoundly impaired in mice overexpressing amyloid precursor protein. *Am J Physiol Heart Circ Physiol*. 2002;283:H315–H323.
18. Franciosi S, De Gasperi R, Dickstein DL, English DF, Rocher AB, Janssen WG, Christoffel D, Sosa MA, Hof PR, Buxbaum JD, Elder GA. Pepsin pretreatment allows collagen IV immunostaining of blood vessels in adult mouse brain. *J Neurosci Methods*. 2007;163:76–82.
19. Cifuentes D, Poittevin M, Dere E, Broqueres-You D, Bonnin P, Benessiano J, Pocard M, Mariani J, Kubis N, Merkulova-Rainon T, Levy BI. Hypertension accelerates the progression of Alzheimer-like pathology in a mouse model of the disease. *Hypertension*. 2015;65:218–224.
20. Brown WR, Thore CR. Review: cerebral microvascular pathology in ageing and neurodegeneration. *Neuropathol Appl Neurobiol*. 2011;37:56–74.
21. Petry FR, Pelletier J, Bretteville A, Morin F, Calon F, Hebert SS, Whittington RA, Planel E. Specificity of anti-tau antibodies when analyzing mice models of Alzheimer's disease: problems and solutions. *PLoS One*. 2014;9:e94251.
22. Nagai K, Akishita M, Machida A, Sonohara K, Ohni M, Toba K. Correlation between pulse wave velocity and cognitive function in nonvascular dementia. *J Am Geriatr Soc*. 2004;52:1037–1038.
23. Scuteri A, Tesauro M, Appolloni S, Preziosi F, Brancati AM, Volpe M. Arterial stiffness as an independent predictor of longitudinal changes in cognitive function in the older individual. *J Hypertens*. 2007;25:1035–1040.
24. Iulita MF, Noriega de la Colina A, Girouard H. Arterial stiffness, cognitive impairment and dementia: confounding factor or real risk? *J Neurochem*. 2018;144:527–548.
25. Braak H, Braak E. Neuropathological stageing of Alzheimer-related changes. *Acta Neuropathol*. 1991;82:239–259.
26. Hanyu H, Sato T, Hirao K, Kanetaka H, Iwamoto T, Koizumi K. The progression of cognitive deterioration and regional cerebral blood flow patterns in Alzheimer's disease: a longitudinal SPECT study. *J Neurol Sci*. 2010;290:96–101.
27. Aries MJ, Elting JW, De Keyser J, Kremer BP, Vroomen PC. Cerebral autoregulation in stroke: a review of transcranial Doppler studies. *Stroke*. 2010;41:2697–2704.
28. Strandgaard S, Olesen J, Skinhoj E, Lassen NA. Autoregulation of brain circulation in severe arterial hypertension. *BMJ*. 1973;1:507–510.
29. den Abeelen AS, Lagro J, van Beek AH, Claassen JA. Impaired cerebral autoregulation and vasomotor reactivity in sporadic Alzheimer's disease. *Curr Alzheimer Res*. 2014;11:11–17.
30. Mankovsky BN, Piolot R, Mankovsky OL, Ziegler D. Impairment of cerebral autoregulation in diabetic patients with cardiovascular autonomic neuropathy and orthostatic hypotension. *Diabet Med*. 2003;20:119–126.
31. Cipolla MJ. *The Cerebral Circulation*. San Rafael, CA: Morgan and Claypool Publishers; 2009.
32. Bolduc V, Drouin A, Gillis MA, Duquette N, Thorin-Trescases N, Frayne-Robillard I, Des Rosiers C, Tardif JC, Thorin E. Heart rate-associated mechanical stress impairs carotid but not cerebral artery compliance in dyslipidemic atherosclerotic mice. *Am J Physiol Heart Circ Physiol*. 2011;301:H2081–H2092.
33. Baraghis E, Bolduc V, Lefebvre J, Srinivasan VJ, Boudoux C, Thorin E, Lesage F. Measurement of cerebral microvascular compliance in a model of atherosclerosis with optical coherence tomography. *Biomed Opt Express*. 2011;2:3079–3093.
34. Bolduc V, Baraghis E, Duquette N, Thorin-Trescases N, Lambert J, Lesage F, Thorin E. Catechin prevents severe dyslipidemia-associated changes in wall biomechanics of cerebral arteries in LDLr-/-:hApoB+/+ mice and improves cerebral blood flow. *Am J Physiol Heart Circ Physiol*. 2012;302:H1330–H1339.
35. Hossmann KA. Glutamate-mediated injury in focal cerebral ischemia: the excitotoxin hypothesis revised. *Brain Pathol*. 1994;4:23–36.
36. Cooper LL, Woodard T, Sigurdsson S, van Buchem MA, Torjesen AA, Inker LA, Aspelund T, Eiriksdottir G, Harris TB, Gudnason V, Launer LJ, Mitchell GF. Cerebrovascular damage mediates relations between aortic stiffness and memory. *Hypertension*. 2016;67:176–182.
37. Poels MM, Ikram MA, van der Lugt A, Hofman A, Krestin GP, Breteler MM, Vernooij MW. Incidence of cerebral microbleeds in the general population: the Rotterdam Scan Study. *Stroke*. 2011;42:656–661.
38. Corrada MM, Sonnen JA, Kim RC, Kawas CH. Microinfarcts are common and strongly related to dementia in the oldest-old: the 90+ study. *Alzheimers Dement*. 2016;12:900–908.
39. Akoudad S, Portegies ML, Koudstaal PJ, Hofman A, van der Lugt A, Ikram MA, Vernooij MW. Cerebral microbleeds are associated with an increased risk of stroke: the Rotterdam study. *Circulation*. 2015;132:509–516.
40. Akoudad S, de Groot M, Koudstaal PJ, van der Lugt A, Niessen WJ, Hofman A, Ikram MA, Vernooij MW. Cerebral microbleeds are related to loss of white matter structural integrity. *Neurology*. 2013;81:1930–1937.
41. Poels MM, Ikram MA, van der Lugt A, Hofman A, Niessen WJ, Krestin GP, Breteler MM, Vernooij MW. Cerebral microbleeds are associated with worse cognitive function: the Rotterdam Scan Study. *Neurology*. 2012;78:326–333.
42. Storck SE, Meister S, Nahrath J, Meissner JN, Schubert N, Di Spiezio A, Baches S, Vandenbroucke RE, Bouter Y, Prikulis I, Korth C, Weggen S, Heimann A, Schwaninger M, Bayer TA, Pietrzik CU. Endothelial LRP1 transports amyloid-beta(1-42) across the blood-brain barrier. *J Clin Invest*. 2016;126:123–136.
43. Montagne A, Barnes SR, Sweeney MD, Halliday MR, Sagare AP, Zhao Z, Toga AW, Jacobs RE, Liu CY, Amezcua L, Harrington MG, Chui HC, Law M, Zlokovic BV. Blood-brain barrier breakdown in the aging human hippocampus. *Neuron*. 2015;85:296–302.
44. Hajjar I, Goldstein FC, Martin GS, Quyyumi AA. Roles of arterial stiffness and blood pressure in hypertension-associated cognitive decline in healthy adults. *Hypertension*. 2016;67:171–175.
45. Oveisgharan S, Hachinski V. Hypertension, executive dysfunction, and progression to dementia: the Canadian Study of Health and Aging. *Arch Neurol*. 2010;67:187–192.
46. Sadekova N, Iulita MF, Vallerand D, Muhire G, Bourmoum M, Claing A, Girouard H. Arterial stiffness induced by carotid calcification leads to cerebral gliosis mediated by oxidative stress. *J Hypertens*. 2018;36:286–298.
47. Lv X, Li W, Luo Y, Wang D, Zhu C, Huang ZX, Tan X. Exploring the differences between mouse mAbeta(1-42) and human hAbeta(1-42) for Alzheimer's disease related properties and neuronal cytotoxicity. *Chem Commun (Camb)*. 2013;49:5865–5867.
48. Jankowsky JL, Younkin LH, Gonzales V, Fadale DJ, Slunt HH, Lester HA, Younkin SG, Borchelt DR. Rodent A beta modulates the solubility and distribution of amyloid deposits in transgenic mice. *J Biol Chem*. 2007;282:22707–22720.
49. Hughes TM, Kuller LH, Barinas-Mitchell EJ, McDade EM, Klunk WE, Cohen AD, Mathis CA, Dekosky ST, Price JC, Lopez OL. Arterial stiffness and beta-amyloid progression in nondemented elderly adults. *JAMA Neurol*. 2014;71:562–568.
50. Hughes TM, Kuller LH, Barinas-Mitchell EJ, Mackey RH, McDade EM, Klunk WE, Aizenstein HJ, Cohen AD, Snitz BE, Mathis CA, Dekosky ST, Lopez OL. Pulse wave velocity is associated with beta-amyloid deposition in the brains of very elderly adults. *Neurology*. 2013;81:1711–1718.
51. Nithianantharajah J, Hannan AJ. The neurobiology of brain and cognitive reserve: mental and physical activity as modulators of brain disorders. *Prog Neurobiol*. 2009;89:369–382.
52. Weiler M, Casseb RF, de Campos BM, de Ligo Teixeira CV, Carletti-Cassani A, Vicentini JE, Magalhaes TNC, de Almeira DQ, Talib LL, Forlenza OV, Balthazar MLF, Castellano G. Cognitive reserve relates to functional network efficiency in Alzheimer's disease. *Front Aging Neurosci*. 2018;10:255.

SUPPLEMENTAL MATERIAL

Data S1.

Supplemental Material

Blood pressure

Animals were acclimated to the testing apparatus during three days prior to blood pressure assessment. Systolic blood pressure was monitored by non-invasive tail-cuff plethysmography (Kent Scientific Corp, USA) two days before the periarterial application of $CaCl_2$ or NaCl (day 0) and weekly for 3 weeks. Following a period of 10 minutes of acclimation, a minimum of 5 measurements were taken until blood pressure stabilized. Following stabilization, 10 measurements were taken per mouse and averaged for analysis. Measurements were taken at the same time of the day by the same experimenter.

Autoradiography

Resting cerebral blood flow (CBF) was measured 2 weeks after the periarterial application of NaCl or $CaCl_2$ in awake mice by quantitative autoradiography, using [^{14}C]IAP (Iodoantipirine 4-N-Methyl-^{14}C, Perkin Elmer, Canada) as a diffusible tracer. Under isoflurane anaesthesia (induction: 5%, maintenance: 2%), the femoral vein was catheterized for tracer infusion. The femoral artery was catheterized for mean arterial pressure monitoring and blood collection. The discomfort caused by the surgery was treated locally with bupivacaine (Marcaine, CDMV, Canada, 4 mg/kg s.c.). Mice were placed in prone position with their head covered and held under minimal restraint. Body temperature was maintained at 37 ºC.

Tracer infusion (1 µCi / 10 g body weight, 8 ml/hour) began two hours after isoflurane anaesthesia was stopped. Arterial blood was collected every 5 seconds during a period of 45 seconds, with the first collection done before tracer infusion. At the end of the 45-second period, mice were decapitated, the brain was quickly removed and frozen in cold isopentane (-30 ºC) for 5-10 seconds

and then stored at -80 ºC until tissue sectioning. Coronal brain sections were cut on a cryostat at 20-µm thickness and mounted on glass slides.

Brain sections and ^{14}C standards (American Radiolabeled Chemicals Inc., USA) were exposed to autoradiography films (Kodak BioMax MR Film, USA) during 10 days for densitometry analysis with the MCID™ Densitometry System software (MCID 7.0, Imaging Research Inc, ON, Canada). Plasma was obtained by centrifugation of peripheral blood at 2000 g for 20 minutes, 4°C. Plasma samples were placed in vials in the presence of scintillating liquid (Ultima Gold, PerkinElmer Inc., USA) and radioactivity was counted using a liquid scintillation counter (1219 RachBeta, LKB Wallac, USA). Radioactivity counts obtained were entered into the MCID™ Densitometry System software according to the sampling time (every 5 seconds). The software calculates CBF as a function of the plasma contamination curve (radioactivity counts in plasma as a function of time) and of the intensity of the ^{14}C standards. Brain sections containing the dorsal hippocampus (from Bregma -1.82 to -2.18 mm) were used for analysis in the following regions: visual and somatosensory cortex (VSCx), perirhinal and entorhinal cortex (PECx), CA1 (cornu ammonis area 1), CA2-3 (cornu ammonis area 2-3), DG (dentate gyrus), thalamic nuclei (THA) and corpus callosum (CC). Four brain sections per animal were examined and data from the right hemisphere (corresponding to the side of the calcified carotid) was used for analysis.

In vivo laser Doppler flowmetry

Cerebrovascular autoregulation and CBF responses to whisker stimulation and to endothelium-dependent and independent vasodilators were examined 2 weeks after the periarterial application of NaCl or $CaCl_2$. Anaesthesia was initiated with isoflurane (induction: 5%, maintenance: 2%) and maintained with alpha-chloralose (50 mg/kg, i.p.) and urethane (750 mg/kg, i.p.). The femoral

artery was cannulated with a heparinized catheter for the monitoring of mean arterial pressure and arterial blood gases. Animals were placed in a stereotax and artificially ventilated through the trachea with a nitrogen/oxygen mixture (Harvard Apparatus, Inspira Advanced Safety Ventilator). Body temperature was maintained at 37 ºC with a thermostatically controlled rectal probe.

For analysis of neurovascular coupling and endothelial CBF regulation, a 2x2 mm cranial window was drilled above the right somatosensory cortex. The pia mater was removed and the exposed area was superfused with artificial cerebrospinal fluid (aCSF) (0.5 mL/min, 35ºC; composition: NaCl 125 mM, KCl 3 mM, $NaHCO_3$ 26 mM, $NaH_2PO_4 \cdot H_2O$ 1.25 mM, $CaCl_2 \cdot 2H_20$ 2 mM, $MgCl_2 \cdot 6H_2O$ 1mM, glucose 4 mM, ascorbic acid 0.4 mM) in the presence or absence of drugs. A laser Doppler probe (AD Instruments, USA) was placed above the whisker barrel area with the aid of a micromanipulator. Analysis of CBF began 30 minutes after the end of the cranial window procedure and subsequent interruption of isoflurane to allow blood gases to stabilise. Blood gases, pH, mean arterial pressure and CBF at baseline before the stimulations were measured to ensure that physiological parameters were comparable between groups (Supplemental Table 1).

Microhemorrages

Microhemorrages were examined with the Prussian blue staining at 3 weeks post-surgery. Brain sections were mounted on microscope slides (Superfrost Plus, Fisher Scientific, USA) and allowed to dry overnight. The next day, they were immersed in a solution of 1% potassium ferrocyanide (Bioshop, Canada) and 1% HCl for 30 minutes. Following this, three washes (5 minutes each) were carried out; two with distilled water and one with tap water followed by immersion in a solution of 1% Neutral Red-1% glacial acetic acid for 2 minutes. Three one-minute washes with tap water were done and the slides were then soaked once in 95% ethanol, once in 100% ethanol

and twice in xylene (5 minutes each) before coverslipping (D.P.X.; Sigma-Aldrich, ON, Canada). Brain sections from a mouse model of hyperhomocysteinemia [1] kindly provided by Dr. Donna Wilcock (University of Kentucky, USA) were used as a positive control of the Prussian blue protocol. Micrographs were acquired with a Leitz Diaplan microscope equipped with an Olympus DP21 camera (Wild Leitz GmbH, Germany).

Aβ40 and Aβ42 ELISA

Endogenous mouse Aβ40 and Aβ42 were measured by ELISA (KMB3481 and KMB3441, Life Technologies, Invitrogen, USA) at 3 weeks post-surgery. Following decapitation, frontal cortex and hippocampus were dissected from the right hemisphere and frozen at -80 ºC until further analysis. Brain tissues were weighed, homogenized in 8X volumes of a guanidine solution (5M guanidine-HCl in 50 mM Tris-HCl, pH 8.0) and incubated 3 hours at room temperature under agitation. Following centrifugation (16,000 g, 20 minutes) the supernatants were recovered and used for analysis (in duplicate). A separate group of mice was used for plasma Aβ quantification. Blood was collected from the cava vein and plasma was obtained by centrifugation in heparinized tubes (2000 g, 20 minutes). Plasma was diluted in half and processed according to the instructions of the manufacturer. Aβ levels in brains were expressed as pmol/g of brain tissue and the ratio Aβ40/42 was calculated.

Tau Western blot

Body temperature was monitored at sacrifice since hypothermia is known to induce tau hyperphosphorylation [2, 3]. Mice were killed by decapitation without anaesthesia, as anaesthesia can increase hypothermia-induced tau phosphorylation [4]. Hippocampal and frontal cortex tissue (right side) were dissected and frozen on dry ice and kept at -80˚C until they were homogenized, without

thawing, in RIPA buffer (50 mM Tris-HCl, pH 7.4, 1% NP-40, 150 mM NaCl, 0.25% Na-deoxycholate, 1 mM EDTA, 1 mM Na_3VO_4, 1 mM NaF, 1 mM PMSF, 10 µl/ml) supplemented with a protease inhibitor cocktail (Sigma-Aldrich, St. Louis, USA). Western blots were done according to our published protocol [5]. The following primary antibodies were used: AT8 (epitopes pSer202/Thr205, Thermo Fisher Scientific, MN1020), CP13 (epitope pSer202, provided by Dr. Peter Davies), PHF-1 (epitopes pSer396, pSer404, provided by Dr. Peter Davies), Tau1 (dephosphorylated epitopes at Ser195, Ser198, Ser199 and Ser202, clone PC1C6, Millipore, MAB34200) and TauC (A0024, Dako Cytomation for total tau). Phospho-tau densitometry signals were normalized to total tau. Densitometry values were obtained with the Image Gauge software (Fujifilm, USA).

Table S1. Analysis of blood gases, mean arterial pressure and basal CBF in laser Doppler flowmetry studies

	NaCl	$CaCl_2$	*p* value
pH	7.36 ± 0.09	7.30 ± 0.03	0.123
pO_2	126.1 ± 7.9	124.7 ± 9.1	0.792
pCO_2	39.8 ± 3.4	42.4 ± 2.3	0.190
Mean arterial pressure	84.0 ± 15.7	69.2 ± 15.6	0.240
CBF at baseline	183.7 ± 44.5	186.0 ± 80.0	0.965

CBF = cerebral blood flow. Data is expressed as mean ± SD and analyzed with a two-tailed Student's t test

Table S2. Quantitative analysis of amyloid-β peptides in brain and plasma

		NaCl	$CaCl_2$	*p* value
Hippocampus	**Aβ40**	174.5 ± 42.2	175.1 ± 31.4	0.9770
	Aβ42	18.9 ± 4.3	17.4 ± 3.3	0.7587
Frontal cortex	**Aβ40**	260.7 ± 51.6	229.4 ± 67.8	0.2949
	Aβ42	26.0 ± 5.0	21.1 ± 6.2	0.1807
Plasma	**Aβ40**	225.7 ± 20.1	236.0 ± 17.8	0.1768
	Aβ42	24.5 ± 1.6	24.9 ± 1.6	0.8147

Concentration is expressed in pg/ml/g tissue and data depicted as mean ± SD. Analysis was done with a two-tailed Student's t test.

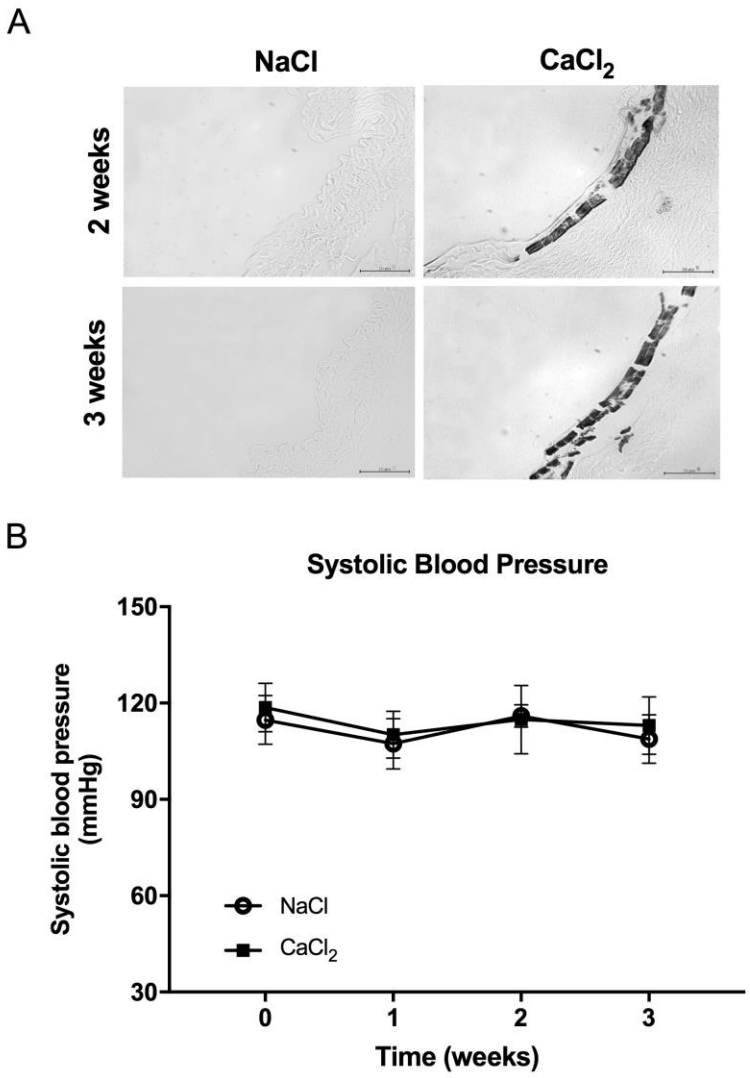

Figure S1. Assessment of calcium deposition and blood pressure. (A) Examination of calcium deposits with the Von Kossa stain at two and three weeks post-calcification in carotid sections from the right hemispheres, in controls (NaCl) and in mice with carotid stiffness ($CaCl_2$). Scale bar = 50 μm. (B) Systolic blood pressure (mmHg) was measured with the tail-cuff method. Graph represents mean ± SD. Data was analyzed with Two Way ANOVA and the Bonferroni correction; *n*=5-8 mice/group.

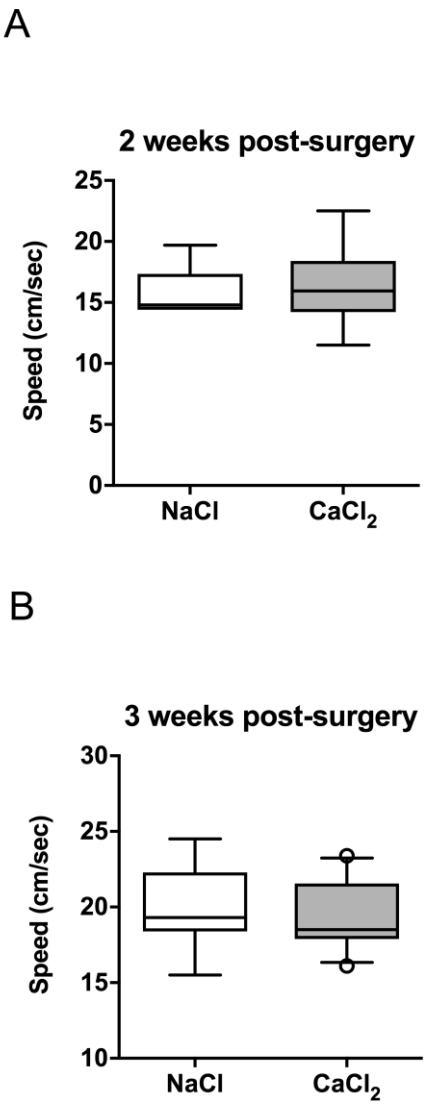

Figure S2. Assessment of locomotor activity. Locomotor activity was evaluated at two (A) and three (B) weeks post-calcification in controls (NaCl) and in mice with carotid stiffness ($CaCl_2$) by comparing the swimming speed (cm/sec) of mice trained in the Morris Water Maze. Data is displayed in box and whiskers plots, where the median is represented by the horizontal line and the 10^{th} and 90^{th} percentiles extend from the extremes of the box. No significant differences, unpaired Student's t-test; 2 weeks (n=8-9); 3 weeks (n=9-13).

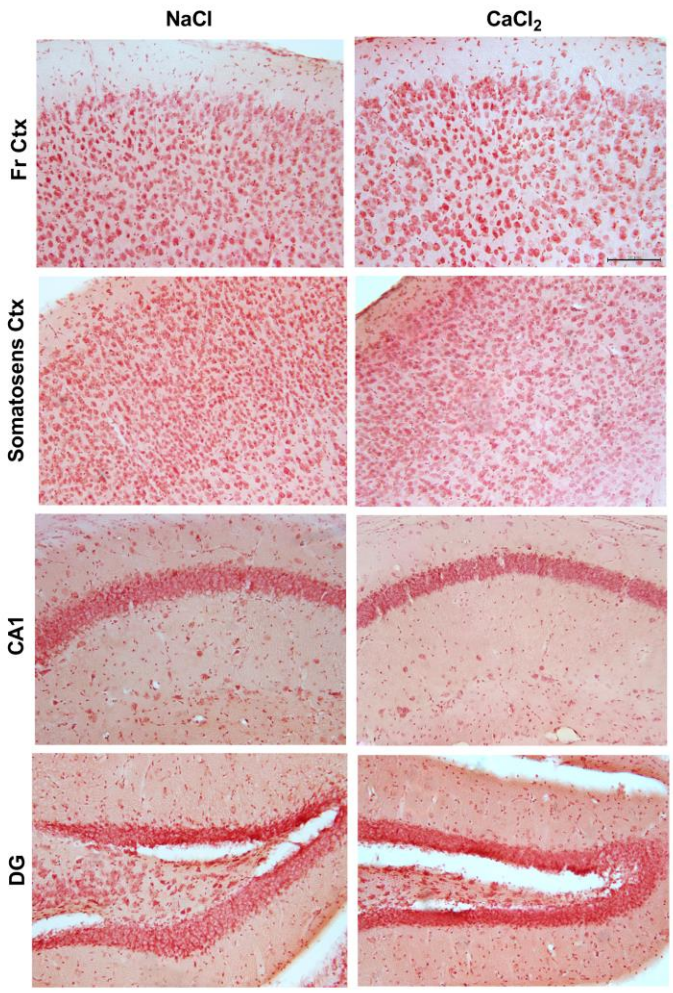

Figure S3. Effect of carotid calcification on cerebral microhemorrages. Microhemorrages were examined with the Prussian blue reaction at 3 weeks post-surgery in brain sections from the right hemispheres, in controls (NaCl) and in mice with carotid stiffness ($CaCl_2$). Tissue was counterstained with 1% Neutral red-1% glacial acetic acid. Fr ctx: frontal cortex; Somatosens ctx: somatosensory cortex; CA1: cornu ammonis 1; DG: dentate gyrus. Scale bar = 50 μm, magnification = 10X, *n*=6/group.

Supplemental References:

1. Sudduth TL, Powell DK, Smith CD , Greenstein A, Wilcock DM. Induction of hyperhomocysteinemia models vascular dementia by induction of cerebral microhemorrhages and neuroinflammation. *J Cereb Blood Flow Metab.* 2013; 33**:** 708-15.

2. Planel E, Miyasaka T, Launey T, Chui DH, Tanemura K, Sato S, Murayama O, Ishiguro K, Tatebayashi Y, Takashima A. Alterations in glucose metabolism induce hypothermia leading to tau hyperphosphorylation through differential inhibition of kinase and phosphatase activities: implications for Alzheimer's disease. *J Neurosci.* 2004; 24**:** 2401-11.

3. El Khoury NB, Gratuze M, Petry F, Papon MA, Julien C, Marcouiller F, Morin F, Nicholls SB, Calon F, Hébert SS, Marette A, Planel E. Hypothermia mediates age-dependent increase of tau phosphorylation in db/db mice. *Neurobiol Dis.* 2016; 88**:** 55-65.

4. Planel E, Richter KEG, Nolan CE, Finley JE, Liu L, Wen Y, Krishnamurthy P, Herman M, Wang L, Schachter JB, Nelson RB, Lau LF, Duff KE. Anesthesia leads to tau hyperphosphorylation through inhibition of phosphatase activity by hypothermia. *J Neurosci.* 2007; 27**:** 3090-3097.

5. Petry FR, Pelletier J, Bretteville A, Morin F, Calon F, Hébert SS, Whittington RA, Planel E. Specificity of anti-tau antibodies when analyzing mice models of Alzheimer's disease: problems and solutions. *PLoS One.* 2014; 9**:** e94251.